Eur Biophys J (2005) 34: 442–453
DOI 10.1007/s00249-005-0479-7

ARTICLE

Wei Qu · Andrew J. Moorhouse · Trevor M. Lewis
Kerry D. Pierce · Peter H. Barry

Mutation of the pore glutamate affects both cytoplasmic and external dequalinium block in the rat olfactory CNGA2 channel

Received: 2 December 2004 / Revised: 21 February 2005 / Accepted: 28 February 2005 / Published online: 1 June 2005

Abstract Dequalinium has recently been reported to block CNGA1 and CNGA2 channels expressed in *Xenopus laevis*. Using the inside-out configuration of the patch-clamp technique, we examined the effects of dequalinium on rat olfactory CNGA2 channels expressed in human embryonic kidney (HEK293) cells and studied aspects of its molecular mechanism of action. We found that cytoplasmic dequalinium blocked wild-type (WT) CNGA2 channels in a voltage-dependent manner with an IC_{50} of approximately 1.3 μM at a V_m of + 60 mV, and an effective fractional charge, $z\delta$, of +0.8 ($z=2$, $\delta=+0.4$), suggesting that cytoplasmic dequalinium interacts with a binding site that is about two fifths of the way along the membrane electric field (from the intracellular side). Neutralizing the negatively charged pore lining glutamate acid residue (E342Q) still allows effective channel block by cytoplasmic dequalinium with an IC_{50} of approximately 2.2 μM at a V_m of +60 mV but now having a $z\delta$ of +0.1 ($\delta=+0.05$), indicating a profoundly decreased level of voltage-dependence. In addition, by comparing the extent of block under different levels of channel activation, we show that the block by cytoplasmic dequalinium displayed clear state-dependence in WT channels by interacting predominantly with the closed channel, whereas the block in E342Q channels was state-independent. Application of dequalinium to the external membrane surface also blocked currents through WT channels and the E342Q mutation significantly increased the IC_{50} for external block approximately fivefold. These results confirm dequalinium as a potent, voltage-dependent and state-dependent blocker of cyclic-nucleotide-gated channels, and show that neutralization of the E342 residue profoundly affects the block by both cytoplasmic and external application of dequalinium.

Keywords P-loop · Channel blockers · Cyclic-nucleotide-gated channels · OCNC1 · CNGα3

W. Qu · A. J. Moorhouse · T. M. Lewis · P. H. Barry (✉)
School of Medical Sciences, The University of New South Wales, Sydney, NSW, 2052, Australia
E-mail: p.barry@unsw.edu.au
Tel.: +61-2-93851101
Fax: +61-2-93851099

K. D. Pierce
Neurobiology Division, The Garvan Institute of Medical Research, Darlinghurst, NSW, 2010, Australia

Introduction

In olfactory receptor neurons, binding of odorants to olfactory receptors induces a rapid increase in cyclic adenosine monophosphate (cAMP), leading to the direct activation of nonspecific cation-selective olfactory cyclic-nucleotide-gated (CNG) channels (Lancet 1986; Zufall et al. 1994). The influx of cations (mainly Na^+ and Ca^{2+}) depolarizes the cell, and the influx of Ca^{2+} ions activates Ca^{2+}-activated Cl channels to further amplify the depolarization (Lowe and Gold 1993; Frings et al. 1995). The CNG channels are considered to belong to the superfamily of tetrameric cation channels whose subunits have six transmembrane domains. Hence, the pore-forming P-region shares sequence similarity with the ion-conducting pore of voltage-gated Shaker-type K^+ channels and with the pore of two-membrane-domain K^+ channels (Kaupp et al. 1989; Jan and Jan 1990; Heginbotham et al. 1992). By analogy with the structure of the pore region of K^+ channels (Doyle et al. 1998), the four P-loops of CNG channel subunits comprise a pore helix directed towards the centre of the channel followed by an uncoiled region which extends back in the extracellular direction, and whose residues form the selectivity filter region of the pore. While there are some functionally significant differences in the selectivity filter sequence (TTVGYGD) of K^+ channels and CNG channels (TTIG–E) a recent model of the CNG pore, derived from cysteine accessibility and homology with KcsA, places the pore glutamate on the external end of the selectivity filter, within the most constricted region of the conduction pathway (Becchetti and coworkers 1999, 2000).

An important approach for identifying pore structure and elucidating any conformational changes that occur in this region during channel gating is to investigate the molecular actions of different pore blockers under different conditions. Reported CNG channel pore blockers include protons, Mg^{2+} and Ca^{2+} as well as more complex molecules such as spermine, pseudechetoxin, pimozide, *l-cis*-diltiazem and tetracaine (Root and MacKinnon 1993; Fodor and coworkers 1997a, 1997b; Lynch 1999; Brown et al. 1999).

Any exposed negative charges near the channel pore represent potential sites of interaction with positively charged blockers of cation channels. A negatively charged glutamate residue in the ion-conducting pathway of CNG channels, tentatively assigned to a position on the extracellular edge of the selectivity filter, is well conserved throughout the superfamily of voltage-gated channels (Heginbotham et al. 1992). This charged pore residue has been shown to form a high-affinity binding site for external protons (Root and MacKinnon 1994), external monovalent and divalent cations (Root and MacKinnon 1993; Eismann et al. 1994; Park and MacKinnon 1995) and externally applied spermine (Nevin et al. 2000). For example, in the bovine rod CNGA1 and olfactory CNGA2 channels, the mutation of this residue into glycine or glutamine dramatically changed the voltage-dependent block by external divalent cations into a weak voltage-independent block, indicating that this position forms the binding site for divalent cations (Root and MacKinnon 1993; Eismann et al. 1994; Park and MacKinnon 1995; Gavazzo et al. 2000). However, neutralization of the glutamate residue did not profoundly affect block by internal divalent cations, suggesting that there is a second, internal cation-binding site (Root and MacKinnon 1993; Gavazzo et al. 2000). The mutation of this pore glutamate into glutamine in the rat olfactory CNGA2 channels also changed the channel block by external spermine from a voltage-dependent into a voltage-independent block. This suggested that this residue may also be the potential binding site for external spermine, and that the mutation has modified this site and/or created a novel-binding site outside the membrane electrical field (Nevin et al. 2000). It was further suggested that multivalent cations, such as spermine, may have a higher affinity for the site than other cations, and hence compete with monovalent cations to bind to the same glutamate site and thereby reduce the permeation rate of other cations (Nevin et al. 2000). However, similar to the results seen for Ca^{2+} and Mg^{2+} block of bovine rod CNGA1 channels, neutralization of the glutamate residue had smaller effects on cytoplasmic spermine block; shifting the voltage-dependence of block to more positive values (by about +40 mV) without changing the magnitude of spermine block (Guo and Lu 2000). Again this suggests that cytoplasmic block is more complex, perhaps suggesting that other cation-binding sites are also involved.

Local anaesthetics can also block cation channels, including CNG channels, and some detailed investigations have been conducted on tetracaine actions. Tetracaine, applied from the cytoplasmic side in rod CNGA1 channels, has been shown to act as a voltage-dependent and state-dependent pore blocker, displaying a three-order higher affinity in the closed state than in the open state (Fodor et al. 1997a). The same glutamate residue (E363 for rod CNGA1 channels) was also considered to be involved in tetracaine block and its neutralization eliminated the state-dependence of block (Fodor et al. 1997b), indicating that access to this residue was state-dependent and suggesting conformational changes to this region occur during channel gating (Bucossi et al. 1996; Flynn et al. 2001). More specifically, it was suggested that E363 forms a binding site for the charged moiety of cytoplasmic tetracaine, and that a conformational change accompanying channel opening moves the glutamate residue away from tetracaine's positive charge or hinders access of tetracaine to the pore (Fodor et al. 1997b).

Taken together, these observations suggest that externally applied divalent and multivalent cationic pore blockers directly interact with this pore glutamate to inhibit monovalent ion permeation (by either shielding the negative charge of the glutamate and/or by steric occlusion of the pore). Mutating this residue changes the electric field around the outer edge of the pore so that, while higher concentrations of blockers can still inhibit permeation, the voltage-dependence of their block is abolished. For internal application of these blockers the role of the glutamate in their mechanism of action is more complex. The voltage- and state-dependence of block by the larger multivalent blockers is altered by mutations to this glutamate, although it is not clear if this is directly due to loss of electrostatic attraction or is secondary to some conformational change reducing blocker access. For block by internal divalent ions glutamate mutations have more modest effects than for block by external divalent ions, suggesting that internal divalent ions block permeation by a mechanism independent of electrostatic attraction to the inner end of the selectivity filter. However, without more detailed knowledge of the state- and voltage-dependence of a range of internal and external blockers (ideally under similar conditions and protocols) it is still too preliminary to be able to incorporate this information into a more precise mechanistic model.

Dequalinium has recently been shown to voltage-dependently inhibit homomeric rod CNGA1 and CNGA2 channels, and heteromeric CNGA1/CNGB1 channels, expressed in *Xenopus oocytes*, with high affinity (Rosenbaum and coworkers 2003, 2004). This divalent organic cation can also inhibit protein kinase C (Rotenberg and Sun 1998) and has been reported to be a potent and selective nonpeptide blocker of the apamin-sensitive small conductance Ca^{2+}-activated K^{+} channels (Castle et al. 1993; Dunn et al. 1996; Strobaek et al. 2000). The dequalinium block was both voltage-dependent and reduced by increasing the concentration of permeant ions, two features characteristic of pore block

(Rosenbaum et al. 2003). While the original study (where dequalinium was pre-equilibrated for long periods at 0 mV) reported state-independence of block (Rosenbaum et al. 2003), a subsequent report (using a wide range of voltages and shorter equilibration times) reported that dequalinium showed a 3–5 times higher affinity for closed channels than that for open channels (Rosenbaum et al. 2004). In this study, we wished to further charaterize dequalinium block of CNG channels. Specifically, we wished to investigate whether extracellular and intracellular dequalinium was a potent blocker of olfactory CNGA2 channels expressed in HEK293 cells, to investigate the voltage- and state-dependence of dequalinium block and to characterize how mutation to the pore lining glutamate affected dequalinium block.

Materials and methods

Transient expression of CNGA2 subunit complementary DNAs in HEK293 cells

The complementary DNA (cDNA) encoding the rat olfactory CNGA2 subunit (a kind gift of Randy Reed, Johns Hopkins University School of Medicine, Baltimore, USA, via Anne Cunningham, Sydney Children's Hospital; equivalent to CNGα3 of Bönigk et al. 1999) was isolated and subcloned into a pCIS expression vector (Gorman et al. 1990). Site-directed mutagenesis was generated using the oligonucleotide-directed polymerase chain reaction method and the successful incorporation of mutations was confirmed by sequencing the cDNA clones. Human embryonic kidney (HEK 293) cells were transfected with plasmid DNA encoding wild-type (WT) or mutant (E342Q) CNGA2 channels, together with a separate plasmid cDNA for the CD4 surface antigen, using a calcium phosphate precipitation protocol (Chen and Okayama 1987). The CD4 antibody-coated polystyrene beads were used as a marker of successfully transfected cells (Dynabeads M-450, Dynal, Oslo, Norway). Transfected cells were kept in Eagle's minimum essential medium in Hank's salts (Trace Biosciences, NSW, Australia) supplemented with 2 mM glutamine and 10% fetal calf serum on poly-D-lysine and collagen (IV) coated coverslips and incubated in 5% CO_2 at 37°C. Cells were used for patch-clamp recordings typically within 24–72 hrs after transfection and only those cells labeled with beads were chosen for experiments.

Solutions

Membrane currents were measured using inside-out, outside-out or whole-cell patch-clamp configurations (Hamill et al. 1981). Unless otherwise indicated, in all experimental procedures, excised patches were bathed in a divalent-cation-free control solution consisting of 145 mM NaCl, 10 mM *N*-2-hydroxyethylpiperazine-*N*-2-ethanesulfonic (HEPES), and 2 mM ethylene glycol-bis(β-aminoethyl ether)-*N*,*N*,*N*′,*N*′-tetraacetic acid (EDTA), titrated to pH 7.4 with 1 M NaOH. This control solution was also used as the pipette solution. For outside-out and whole-cell recordings, 1 mM cAMP (Sigma–Aldrich; St. Louis, MO, USA) was added to this pipette solution. All the pipette solutions were filtered (with a 0.2-μm filter, Gelman Sciences, Ann Arbor, MI, USA) prior to use. For bath application, different concentrations of cAMP and/or dequalinium were added directly to this control solution, and applied to the excised patches using a continuous flow, multibarrel, gravity-fed, perfusion system consisting of ten adjacent and parallel capillary polyethylene tubes. The patches or cells were positioned right in front of the outflow of the parallel perfusion tubes at a distance of approximately 100 μm. The stock solution of dequalinium chloride [quinolinium, 1,1′-(1,10-decanediyl)bis(4-amino-2-methyl dichloride)] was dissolved in dimethylsulfoxide at a concentration of 4 mM, and stored at room temperature. The final solutions were prepared by diluting this stock solution to between 10 nM and 8 μM with the control solution.

Electrophysiological recording

All experiments were performed at a room temperature of 21 ± 1°C. Recording electrodes were fabricated using standard techniques (Hamill et al. 1981; Corey and Stevens 1983) from filamented, borosilicate glass capillaries (GC150F-15; 1.5-mm outer diameter × 0.86-mm inner diameter, Harvard Apparatus, Kent, UK), using a Flaming/Brown micropipette electrode puller (model P-87, Sutter Instruments, Novato, CA, USA). The tip of the pipette was then fire-polished to give a pipette resistance of 3–5 MΩ. Currents were low-pass-filtered at 2 kHz and sampled at 10 kHz using an Axopatch 1D patch-clamp amplifier (Axon Instruments, Foster City, CA, USA). Currents were measured in response to a series of 200-ms voltage pulses (between −80 and +80 mV, in increments of 20 mV and from a holding potential of 0 mV). Current–voltage (*I*–*V*) relationships were obtained by plotting the average steady-state currents in various test solutions against membrane potentials. Each patch was perfused by a solution containing dequalinium for more than 2 min in order to produce a stable response. For inside-out patches, leak currents in the absence of cyclic nucleotides at the corresponding voltages were subtracted from currents in the presence of cAMP. For outside-out patches we only used recordings in which the high-resistance seal was still apparent immediately after patch excision, and showed a gradual increase in holding current, which saturated after 1–2 mins, reflecting the activation of CNG channels as cAMP diffused to the pipette tip. For whole-cell recordings, data were recorded only from cells whose input resistance gradually decreased after going whole-cell, as cAMP in the pipette diffused

into the cell and activated CNG channels. In addition, we only used whole-cell currents in which the bath application of spermine (1 mM) almost totally blocked the inward currents. When mean values are quoted from a number of measurements, they are given as the mean ± the standard error of the mean. Differences between mean values were analyzed using Student's paired *t* test for paired experiments, and significance was assessed at a *p* value of less than 0.05.

Data analysis

Off-line analysis and graphing of current traces was conducted using pCLAMP 8.0 (Axon Instruments, Foster City, CA, USA) and Sigmaplot (Jandell Scientific, San Rafael, CA, USA) on a Pentium III computer. Concentration–response curves for cAMP were generated by measuring the current response at ±60 mV at different cAMP doses and this relationship was then fitted with the Hill equation:

$$I_{\text{norm}} = C^h / \left(C^h + \text{EC}_{50}^h\right), \tag{1}$$

where I_{norm} is the normalized current amplitude (I/I_{max}), C the cAMP concentration, EC_{50} the concentration of cAMP that gives 50% of the maximal response, and h is the Hill coefficient. The inhibitory dose–response curves for cytoplasmic dequalinium were fitted to a similar Hill-type equation:

$$I_{\text{Deq}}/I_{\text{max}} = I_{\text{offset}} + \left\{ [\text{Deq}]^h \Big/ \left([\text{Deq}]^h + \text{IC}_{50}^h \right) \right\}, \tag{2}$$

where I_{Deq} is the current in the presence of dequalinium, I_{max} is the current obtained in the absence of dequalinium, I_{offset} is the residual unblocked current at maximal dequalinium concentrations, [Deq] represents the concentration of dequalinium applied to the patch from either the cytoplasmic or the external side, IC_{50} is the concentration of dequalinium which results in an inhibition equal to 50% of the maximal inhibition and h is the appropriate Hill coefficient. Note that in Eq. 2, we have allowed for the possibility that in some cells the maximum block was not 100% by adding an offset, I_{offset}.

To describe the voltage-dependence of the dequalinium block of CNG channels, the patches were stepped from a holding potential of 0 mV to between −80 and 80 mV, in increments of 20 mV, for 2 min until steady-state block was reached. A modified Boltzmann equation (Eq. 3) was used to fit the relationship between the membrane voltage and the normalized current amplitudes ($I_{\text{Deq}}/I_{\text{max}}$) in the presence of cytoplasmic dequalinium. The normalized current amplitude was calculated by dividing the steady-state currents recorded in the presence of dequalinium (I_{Deq}) by the maximum cAMP-activated current in the absence of dequalinium (I_{max}) (Rosenbaum et al. 2004).

$$I_{\text{Deq}}/I_{\text{max}} = 1/\{1 + \exp[z\delta(V_{\text{m}} - V_{1/2})F/RT]\}, \tag{3}$$

where $V_{1/2}$ is the voltage when the current reaches half of the maximum activation, V_{m} the membrane potential, z the valence of the blocker, δ the fraction of the membrane electric field from the intracellular or the extracellular side that affects the binding interaction of the blocker to the channel, and R, T and F are the ideal gas constant, the absolute temperature and the Faraday constant, respectively.

To determine the state-dependence of cytoplasmic dequalinium block, the kinetics schemes in Schemes 1, 2, 3 and 4 were fitted to the data.

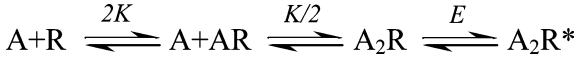

Scheme 1 Linear kinetics scheme (in the absence of block)

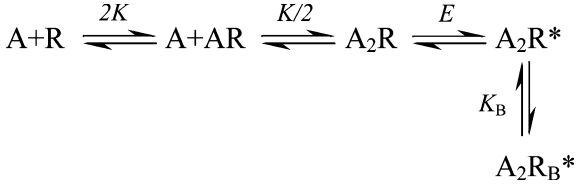

Scheme 2 Open-channel block

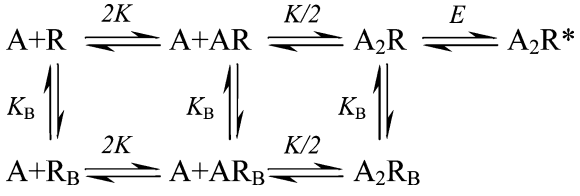

Scheme 3 Closed-channel block

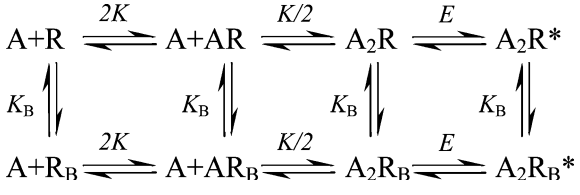

Scheme 4 State independent block

In each kinetics scheme, A is the agonist, R is the receptor-channel complex, R_B is the blocked receptor-channel complex and an asterisk indicates the open state of the receptor channel. The kinetics schemes assume that two molecules of agonist bind to equivalent sites on the receptor before it is able to open. For each of the schemes the macroscopic equilibrium constants are shown, with K being the equilibrium dissociation constant for the agonist cAMP, K_B being that for the blocker dequalinium and E is the equilibrium constant

for the opening reaction (defined as the ratio of the opening rate constant to closing rate constant).

Results

Voltage-dependence of cytoplasmic dequalinium block

Inside-out excised patch-clamp recordings were used for examining the blocking effects of cytoplasmic dequalinium in both WT and E342Q mutant CNGA2 channels. For each concentration of cytoplasmic dequalinium, the patches were perfused with the test solutions for more than 2 min in order to obtain steady-state recordings. Cytoplasmic dequalinium was a potent inhibitor of both WT CNGA2 and mutant E342Q CNGA2 channels, particularly at positive membrane potentials. The block was fully reversible, although washout was slow and required 20–30 min for almost complete recovery (Fig. 1A, B). Examples of current–voltage curves in the presence of different cytoplasmic dequalinium concentrations are shown in Fig. 1C (WT) and D (E342Q), with the voltage-dependence of block at submaximal concentrations of dequalinium also shown in Fig. 2C.

For WT CNGA2 channels, a dramatic block of current was seen at positive membrane potentials, but at negative potentials the extent of block decreased and was negligible at −80 mV. The corresponding current–voltage curves displayed clear inward rectification at a higher concentration of dequalinium, indicating that cytoplasmic dequalinium blocked the cAMP-activated currents more prominently and efficiently at depolarized membrane potentials (Fig. 1C, Table 1). In the presence of 4 μM cytoplasmic dequalinium, the normalized steady-state current amplitude (I_{Deq}/I_{max}) was 0.1 ± 0.03 at a V_m of +60 mV, and 0.9 ± 0.03 at a V_m of −60 mV ($n = 11$). This result is consistent with the idea that dequalinium binds to a site within the membrane electric field.

The *I–V* curves for the E342Q channels showed a different pattern, both in the absence and in the presence of dequalinium (Fig. 1D). The control *I–V* curve showed quite marked outward rectification, which became more linear with increasing concentrations of dequalinium.

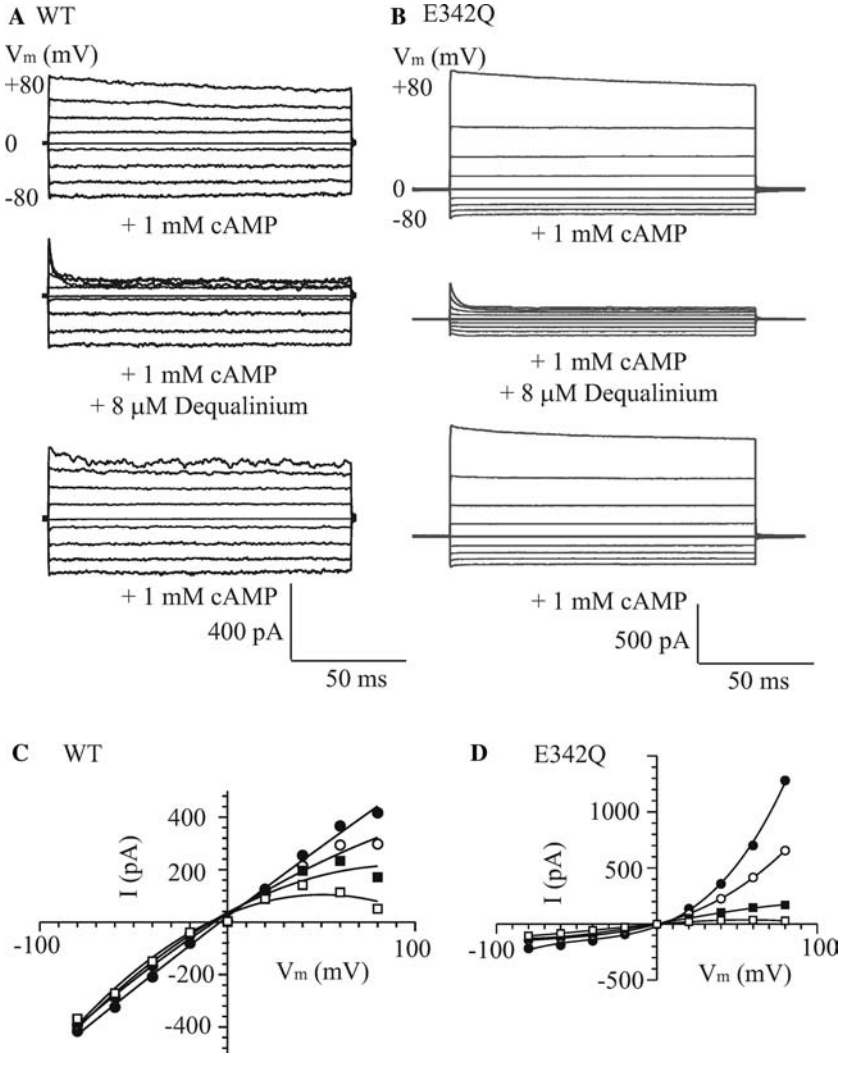

Fig. 1 Block of cyclic adenosine monophosphate (*cAMP*)-activated currents by cytoplasmic dequalinium in wild type (*WT*) and E342Q mutant CNGA2 channels. **A**, **B** Dequalinium reversibly blocked macroscopic currents in both WT and E342Q channels. Currents were measured in response to a series of 180-ms voltage steps ranging from −80 to +80 mV in 20-mV steps, from a holding potential of 0 mV. **C**, **D** Corresponding current–voltage (*I–V*) relations for the currents shown in **A** and **B**. *Filled circles* no dequalinium; *empty circles* 1,000 nM (WT) or 1,600 nM (E342Q) dequalinium; *filled squares* 4 μM dequalinium; *empty squares* 8 μM dequalinium. The *smooth lines* were obtained by fitting the data to quadratic polynomials

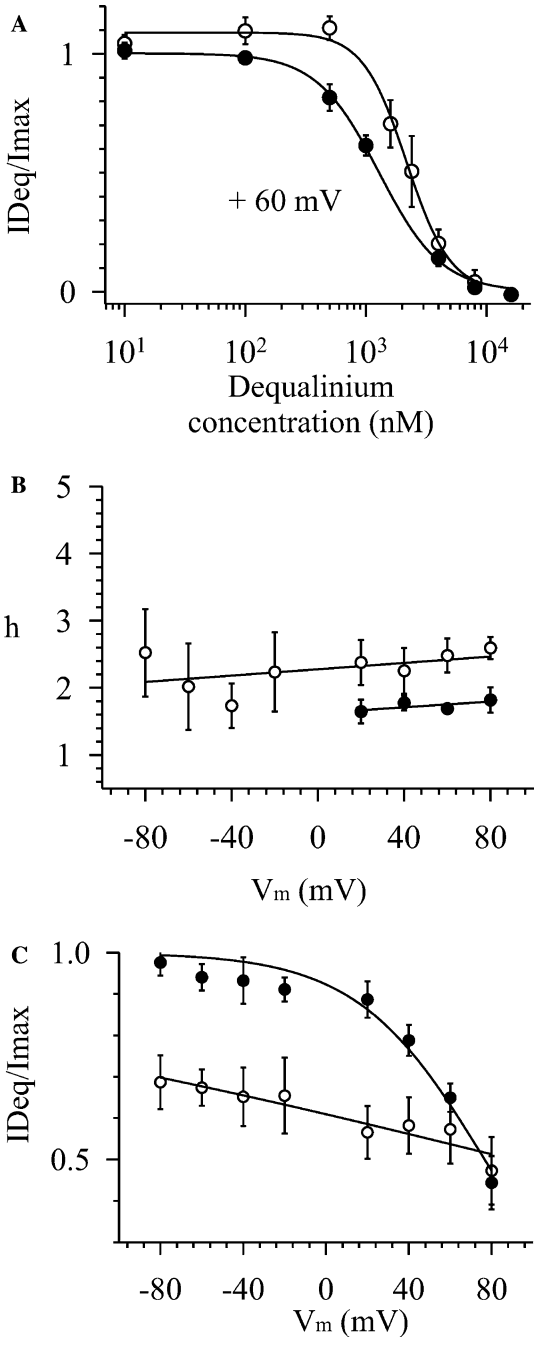

Fig. 2 Comparison of voltage-dependence of cytoplasmic dequalinium block between WT (*filled circles*) and E342Q mutant (*empty circles*) CNGA2 channels activated by saturating concentrations of cAMP. **A** Concentration–response curves for cytoplasmic dequalinium block at a V_m of +60 mV. The *smooth curve* is a fit with the Hill equation (Eq. 2), giving an IC_{50} of 1.3 ± 0.1 μM, and $h = 1.7 \pm 0.1$ for WT ($n = 11$), and an IC_{50} of 2.2 ± 0.1 μM, and $h = 2.4 \pm 0.3$ for E342Q ($n = 7$). **B** Relationship between the Hill coefficient of dequalinium block (inhibition) and membrane potentials. The h values for both WT (*filled circles*) and E342Q mutant (*open circles*) channels were larger than 1 at all voltages. **C** Mean normalized currents (I_{Deq}/I_{max}) in the presence of 1 mM cAMP and 1,000 nM dequalinium in WT channels ($n = 5$), or in the presence of 1 mM cAMP and 1,600 nM dequalinium in E342Q channels ($n = 5$), against voltage. The *smooth line* is a fit to the Boltzmann equation (Eq. 3), giving a $z\delta$ value of 0.8 and a $V_{1/2}$ of about 77 mV for WT channels, and a $z\delta$ value of 0.1 and a $V_{1/2}$ of approximately 90 mV for E342Q channels

Outward rectification of macroscopic currents has been seen with a range of mutations to neutralize the pore glutamate in CNGA1 and CNGA2 channels (Root and Mackinnon 1993; Gavazzo et al. 2000). Gavazzo et al (2000) suggested the rectification of CNGA2 channel currents was solely due to changes in the voltage dependence of ion permeation, while Root and Mackinnon (1993) suggested for the CNGA1 channel that changes in the voltage-dependence of gating also contributed to the macroscopic current rectification. While there was some mild inward rectification at the highest dequalinium concentrations, the inward currents were also reduced by dequalinium in the E342Q mutation. In the presence of 4 μM dequalinium, the value of I_{Deq}/I_{max} was 0.2 ± 0.04 at a V_m of +60 mV, and 0.45 ± 0.05 at a V_m of −60 mV ($n = 5$).

Figure 2A shows the averaged dequalinium concentration–response relationship of WT and E342Q channels at a V_m of +60 mV. The mutation of E342Q shifted the curve slightly towards the right in the presence of a saturating concentration of cAMP, compared with the case for the WT. The fit of the Hill equation to these data gave an IC_{50} for dequalinium of 1.3 ± 0.1 μM and a Hill coefficient (h) of 1.7 ± 0.1 for WT channels ($n = 11$), and an IC_{50} of 2.2 ± 0.1 μM and an h value of 2.4 ± 0.3 for E342Q channels ($n = 7$; Fig. 2A, Table 1). The Hill coefficients obtained from similar fits to dequalinium block data were larger than 1 at all membrane potentials for both WT and E342Q channels (Fig. 2B), suggesting that more than one dequalinium molecule may be concurrently involved in interacting with the channel.

The voltage-dependence of the extent of block induced by a submaximum concentration of dequalinium (1 μM for WT, 1.6 μM for E342Q) is shown in Fig. 2C, and the smooth lines are the fit obtained with the Boltzmann equation (Eq. 3). The data clearly indicate a strong voltage-dependent block in WT channels and only a weak voltage-dependence of block for the E342Q mutant. There was no evidence that dequalinium acted as a permeant blocker within these voltage ranges since we saw no relief from block at +80 mV. The fitting with the Boltzman equation (Eq. 3) gave a $V_{1/2}$ of about 77 mV, and a mean $z\delta$ value of approximately 0.8 in WT channels, and a $V_{1/2}$ of 90 mV and a $z\delta$ value of about 0.1 in E342Q channels. Assuming that both positive charges of dequalinium contribute to the binding reaction, the δ value for the WT channel is estimated to be around 0.4, and the value for the E342Q mutant channel to be about 0.05. These results suggest that cytoplasmic dequalinium blocked the WT channel in a voltage-dependent way with the binding site located approximately two fifths of the way along the membrane electric field from the internal side, whereas the E342Q mutation profoundly disrupted the interaction between dequalin-

Table 1 Parameters for cytoplasmic and external dequalinium block in wild-type (*WT*) and E342Q channels at membrane potentials of +60 and −60 mV

		$1-(I_{4\ \mu M\ Deq}/I_{cAMP})$[a]		IC_{50} (μM)		*h*	
		+60 mV	−60 mV	+60 mV	−60 mV	+60 mV	−60 mV
Cytoplasmic application	WT ($n=11$)	0.9 ± 0.03	0.1 ± 0.03	1.3 ± 0.1	–	1.7 ± 0.1	–
	E342Q ($n=7$)	0.8 ± 0.06	0.5 ± 0.04	2.2 ± 0.1	1.4 ± 0.1	2.4 ± 0.3	2.0 ± 0.6
External application	WT ($n=4$)	0.6 ± 0.07	0.6 ± 0.1	0.4 ± 0.1	0.4 ± 0.1	0.8 ± 0.1	1.1 ± 0.2
	E342Q ($n=3$)	0.1 ± 0.1	0.4 ± 0.2	7.8 ± 4.5	2.6 ± 0.8	1.6 ± 0.4	3.2 ± 0.3

IC_{50} is the concentration of dequalinium which reduces the response to 50% of the maximal response, and *h* is the appropriate Hill coefficient

[a]The fraction of the blocked currents in the presence of 4 μM dequalinium

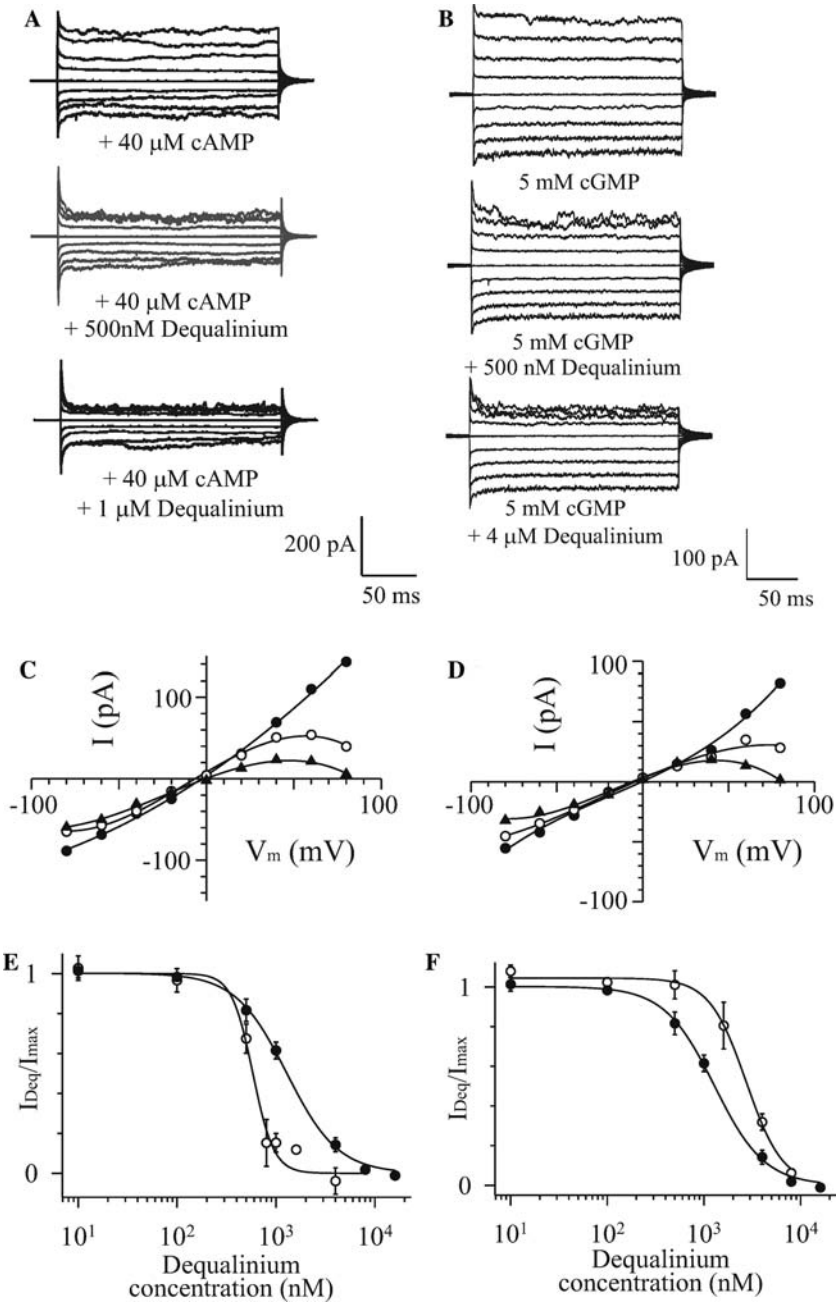

Fig. 3 State-dependent block of cytoplasmic dequalinium in WT CNGA2 channels at subsaturating cAMP and saturating cyclic guanosine monophosphate (*cGMP*) concentrations.
A, **B** Representative currents activated by 40 μM cAMP and 5 mM cGMP in individual inside-out patches.
C, **D** Corresponding *I–V* curves. *Filled circles* 40 μM cAMP (**C**) or 5 mM cGMP (**D**) + no dequalinium; *empty circles* +500 nM dequalinium; *filled triangles* 1,000 or 4,000 nM dequalinium.
E, **F** Concentration–response curves for dequalinium block at a V_m of +60 mV in the presence of 1 mM cAMP (*filled circles* in both **E** and **F**) and in the presence of 40 μM cAMP (*empty circles* in **E**) and in the presence of 5 mM cGMP (*empty circles* in **F**). The *smooth curves* are fits with the Hill equation (Eq. 2), giving an IC_{50} for dequalinium block in the presence of 1 mM cAMP of 1.3 ± 0.1 μM ($n=6$), 0.58 ± 0.05 μM in the presence of 40 μM cAMP ($n=5$), and 2.7 ± 0.1 μM in the presence of 5 mM cGMP ($n=5$)

ium and its binding site. The results clearly indicated that the E342Q mutation converts dequalinium from being a voltage-dependent blocker to being an essentially voltage-independent blocker.

State-dependence of cytoplasmic dequalinium block

We next examined whether cytoplasmic dequalinium block showed any state dependence. The first way we examined this was to determine dequalinium block when activating CNGA2 channels to differing extents, with a subsaturating concentration of cAMP (40 μM) that elicits responses 20–50% of maximal, a saturating concentration of cAMP (1 mM) and a saturating concentration of cyclic guanosine monophosphate (cGMP) (5 mM). In the presence of saturating cGMP the channel open probability (P_o) is 0.996–0.997, while for saturating cAMP P_o is 0.9–0.985 (Gordon and Zagotta 1995; Fodor et al. 1997a; Gavazzo et al. 2000). This difference in the time spent in the open state in saturating cAMP compared with saturating cGMP was sufficient to significantly affect the potency of another proposed pore blocker, tetracaine (Fodor et al. 1997a). Figure 3A and B shows sample current recordings of dequalinium block of currents activated by a subsaturating cAMP concentration (40 μM), and a saturating cGMP concentration (5 mM), and the corresponding *I–V* curves are shown in Fig. 3C and D. Cytoplasmic dequalinium was most potent when the channels were activated by subsaturating cAMP. Dequalinium (1 μM) reduced currents activated by 1 mM cAMP to 0.62 ± 0.04 ($n = 5$) and reduced currents activated by subsaturating (40 μM) cAMP to 0.15 ± 0.05 ($n = 5$) at a membrane potential of +60 mV. This extent of reduction was significantly different. The same concentration of dequalinium had very little effect on currents activated by saturating (5 mM) cGMP (Fig. 3F). Figure 3E and F shows mean concentration–response curves for dequalinium block of currents activated by subsaturating cAMP (Fig. 3E) and saturating cGMP (Fig. 3F). In both cases the curve for inhibition of currents activated by saturating (1 mM) cAMP is shown for comparison. For currents activated by 40 μM cAMP, the dequalinium IC_{50} was 0.58 ± 0.05 μM ($n = 5$), which is significantly less than that for currents activated by 1 mM cAMP (1.3 ± 0.1 μM, $n = 11$, $p < 0.05$). The dequalinium IC_{50} for currents activated by saturating cGMP was even larger, being 2.7 ± 0.1 μM ($n = 5$). These results indicate that cytoplasmic dequalinium is a state-dependent blocker of CNGA2 channels, being more potent when the channel is in the closed state.

To further investigate the state-dependency of dequalinium block of WT and E342Q channels, we used a second approach. The extent of block by a set (approximate IC_{50}) concentration of dequalinium was determined for a range of cAMP concentrations. Figure 4 shows cAMP concentration–response curves in the absence and presence of 1 μM dequalinium (for WT) or 2 μM dequalinium (for E342Q) at a membrane potential of +60 mV. In each case the data were fitted with simple kinetics schemes (Schemes 1, 2, 3, 4; see earlier) that

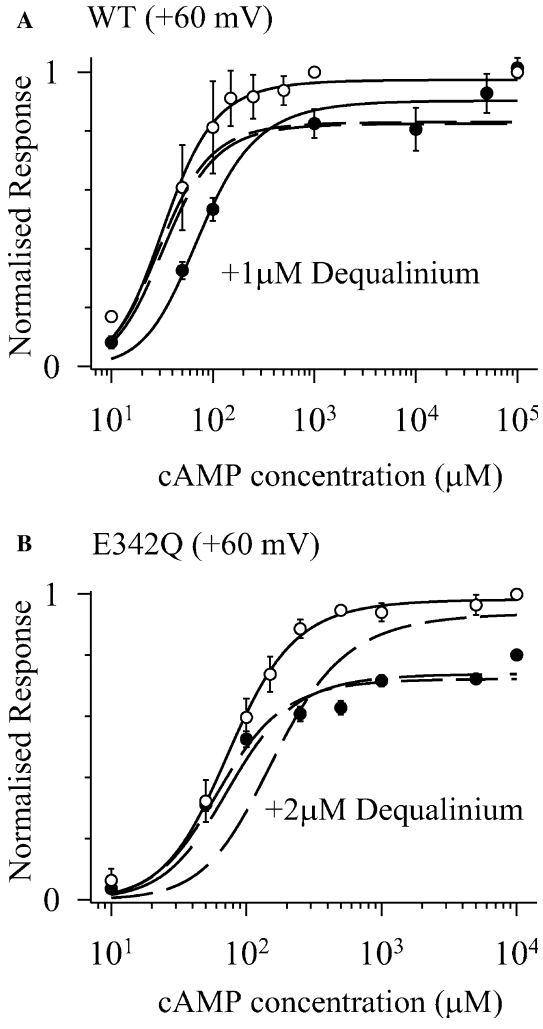

Fig. 4 The effect of cytoplasmic dequalinium at a concentration of about half-maximal block at different concentrations of cAMP in WT and E342Q channels. All currents were measured at +60 mV. **A**, **B** Concentration–response relations in the absence (*empty circles*) and in the presence (*filled circles*) of 1 μM (WT) or 2 μM (E342Q) cytoplasmic dequalinium. The concentration–response curves obtained in the absence of dequalinium were fitted (shown as a *solid line*) with the linear kinetics scheme (Scheme 1) to estimate the values for *K* and *E* from the data. For the WT channel the values obtained were $E = 36 \pm 21$ and $K = 177 \pm 71$ μM^{-1}, and for the E342Q channel $E = 58 \pm 25$ and $K = 509 \pm 137$ μM^{-1}. These parameters were then fixed for fitting of the state-dependent blocking mechanisms so that the only free parameter was K_B for dequalinium. For the WT channel in the presence of 1 μM dequalinium the data were best fit with the closed-state block mechanism (shown as a *smooth curve*; $K_B = 0.34 \pm 0.08$ μM^{-1}) compared with the other two mechanisms (shown as *dashed lines*). The data for E342Q in the presence of 2 μM dequalinium were not fit at all well with the closed-state block mechanism (shown as *shortest dashed line*), but it was not possible to distinguish between the fits for open-state block ($K_B = 5.5 \pm 0.6$ μM^{-1}) or state-independent block ($K_B = 6.1 \pm 0.8$ μM^{-1}; both shown as *longer dashed lines*)

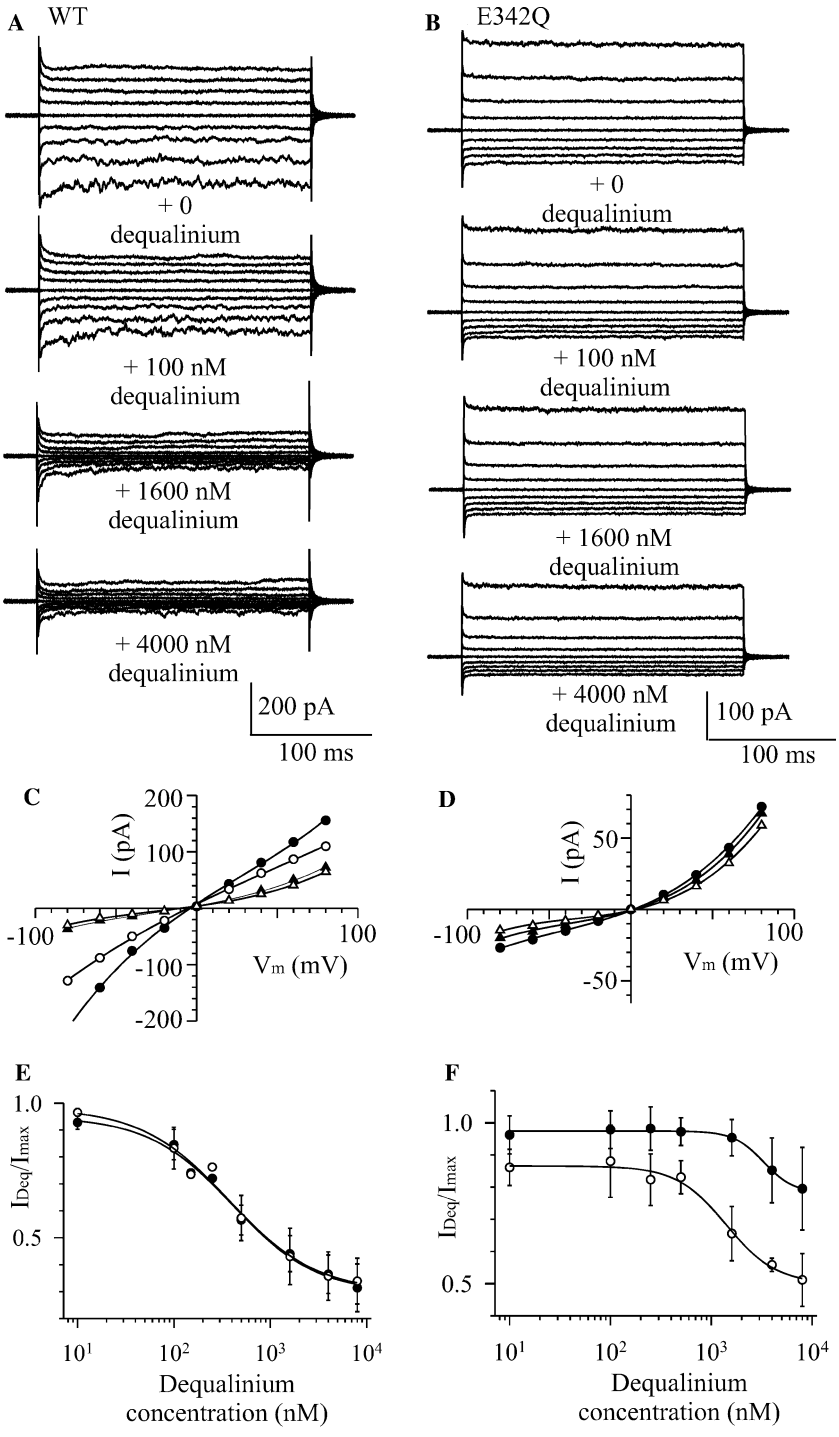

Fig. 5 Effects of external dequalinium on WT and E342Q CNGA2 channels. **A**, **B** Representative dequalinium inhibition in individual outside-out patches containing WT or E342Q channels. The currents were activated by 1 mM cAMP and elicited by a series of potentials from −80 to +80 mV at 20-mV intervals. These currents have not been leakage-subtracted. **C**, **D** Corresponding *I–V* curves: *filled circles* no dequalinium; *empty circles* 100 nM dequalinium; *filled triangles* 1,600 nM dequalinium; *empty triangles* 4,000 nM dequalinium. **E**, **F** The fraction of unblocked currents (I_{Deq}/I_{max}) at a V_m of +60 mV (*filled circles*) and −60 mV (*empty circles*) against the membrane potential. The *smooth lines* are the fit with the Hill equation (Eq. 2). At −60 mV, $IC_{50}\approx372$ nM, $h\approx1.1$ for WT ($n=4$), and $IC_{50}\approx2.6$ μM, $h\approx3.2$ for E342Q channels ($n=3$); at +60 mV, $IC_{50}\approx405$ nM, $h\approx0.8$ for WT, and $IC_{50}\approx7.8$ μM, $h\approx1.6$ for E342Q channels (Table 1)

describe channel activation, open-state block, closed-state block or state-independent block. The scheme we used for describing the state-dependence of dequalinium block assumes two equivalent binding sites for cAMP that need to be occupied before the channel undergoes a concerted opening transition (Gordon and Zagotta 1995; Rosenbaum et al. 2003). The results indicated that the concentration–response curve of

WT channels in the presence of 1 μM dequalinium was best fitted by a kinetics scheme for a closed-state block mechanism (Fig. 4A), whereas for E342Q this was not the case. The E342Q data were best fit by the open-state and state-independent blocking mechanisms and it was not possible to distinguish between these fits (Fig. 4B). This indicates that the neutralization of the negative charge at the E342 position removes the closed

state dependence of the channel block by cytoplasmic dequalinium.

External dequalinium block

The effects of extracellular dequalinium were investigated in outside-out, or whole-cell patch-clamp configurations, in which 1 mM cAMP was included in the pipette solution to activate CNGA2 channels. External dequalinium produced a block of both WT and E342Q CNGA2 channels that reached a steady level within about 5 min. Representative currents (without subtraction of leakage currents) recorded at different dequalinium concentrations in WT and E342Q channels are shown in Fig. 5A and B. External dequalinium still behaved as a potent inhibitor of WT CNGA2 channels, and, in this example, the block was slightly more efficient at more hyperpolarized potentials, as illustrated by the slight outward rectification seen in the corresponding *I–V* curves at high concentrations of dequalinium (Fig. 5C). Mutation of E342 reduced the effectiveness of external dequalinium block, increasing the value of I_{Deq}/I_{max} in the presence of 1,600 nM external dequalinium at a V_m of −60 mV from 0.4 ± 0.1 for WT ($n = 4$) to 0.7 ± 0.1 for E342 ($n = 3$). The fitting of the concentration–response curves of external dequalinium block with the Hill equation (Eq. 2) also illustrates the reduced maximum block and shows the significant reduction in the potency of external dequalinium block in the E342Q channel (Fig. 5E, F, Table 1). While we selected recordings in which background leak seemed minimal (see "Materials and methods"), we cannot discount the possibility that the residual dequalinium resistant current may include a small leak component, resulting in a slight underestimation of maximal block. The dequalinium IC_{50} at −60 mV was 0.4 ± 0.1 μM for WT ($n = 4$) and 2.6 ± 0.8 μM for E342Q ($n = 3$; $p < 0.05$; Table 1); at +60 mV the respective IC_{50} values were 0.4 ± 0.1 μM for WT ($n = 4$) and 7.8 ± 4.5 μM for E342Q ($n = 3$). Hence the E342Q mutation reduces the potency of external dequalinium block and, interestingly, seems to induce some voltage-dependence to the dequalinium block. The mean Hill coefficients for external block were close to 1 and voltage-independent for WT channels, and increased from around 1 (at negative V_m) to over 3 at more depolarized potentials (Table 1). These results suggest that different binding mechanisms are involved for the two types of channels, and that neutralization of the P-loop glutamate has a profound effect on the action of externally applied dequalinium.

Discussion

In this study, we have explored the underlying mechanisms and molecular determinants of dequalinium block of rat olfactory CNG channels. Cytoplasmic dequalinium voltage-dependently and state-dependently blocks WT CNGA2 channels. It was more effective at subsaturating cAMP concentrations when the channel spends more time in the closed state, and less effective at saturating cGMP when the channel spends more time in the open state, indicating a higher affinity for the closed state. Our results with CNGA2 channels in HEK cells correspond well with the potency and voltage-dependence of cytoplasmic dequalinium block of CNGA2 channels expressed in *X. laevis* (Rosenbaum et al. 2003; 2004). Our results with state-dependency also concur with the more recent results obtained in *X. laevis* oocytes (Rosenbaum and coworkers 2004), although no state-dependency of dequalinium block was found in CNGA1 channels expressed in *X. laevis* oocytes after prolonged pre-equilibration at 0 mV (Rosenbaum et al. 2003). However, the results with extracellular dequalinium display some differences from those reported by Rosenbaum et al. (2003). In that study, extracellular dequalinium caused a very slow block that was not complete even after 25 min. As the block was relieved at negative membrane potentials it was suggested that external dequalinium entered the oocyte and blocked from the inside. Our results indicate that extracellular dequalinium blocks via a mechanism distinct from cytoplasmic dequalinium, since external block was rather voltage-independent and the effects of the E342Q mutation on external and cytoplasmic block were quite different (see the following).

Neutralization of the negatively charged pore glutamate residue, by mutation to glutamine (E342Q), markedly reduced the effectiveness of external dequalinium in blocking CNGA2 channels. The analogous residue in CNGA1 channels provides a binding site for external Ca^{2+} and Mg^{2+}, and mutations to neutralize its charge markedly reduced the effectiveness of divalent cations to inhibit channel current (Root and MacKinnon 1993; Eismann et al. 1994). The same E342Q mutation in CNGA2 channels eliminated the voltage-dependent component of extracellular spermine block (Nevin et al. 2000). Our results indicate that this pore glutamate is also integral to potent blocking actions of extracellular dequalinium, and suggest that it contributes to a binding site for a diverse range of cationic channel blockers when applied extracellularly.

The E342Q mutation also changed the mode of block of internal dequalinium into one that was voltage-independent and state-independent. In the WT CNGA2, cytoplasmic dequalinium only produced a significant block at positive membrane potentials with the potency of block being greater when the channels spent a greater proportion of time in the closed state. A similar pattern of behavior was seen with the intracellular tetracaine block of rod CNG channels (CNGA1) expressed in *Xenopus* oocytes with the affinity of WT channel current block by dequalinium being greater in the closed state and the state-dependency being abol-

ished by mutations to neutralize the pore glutamate (E363G; Fodor et al. 1997b). The blocking actions of intracellular spermine were somewhat different from those of dequalinium and tetracaine in that the spermine block is more effective in the open state, and the E342Q mutation does not result in a loss of voltage-dependence, but shifted its sensitivity to block to more positive values (Guo and Lu 2000; although the same mutation did abolish voltage-dependence of extracellular spermine block; Nevin et al. 2000). Hence, for both tetracaine and dequalinium, the pore glutamate underlies the state-dependency of block. Fodor et al (1997b) suggested that the positive charge on tetracaine interacts with the negative carboxy group of the glutamate side-chain, so that when the channel opens the glutamate side chain moves away from the channel pore or else the open pore hinders access of tetracaine to the glutamate. Ghatpande et al. (2003) further speculate that the amino group of tetracaine (and derivatives) interacts with the charged glutamates, while the aromatic, hydophobic end gets stuck in the pore preventing tetracaine acting as a permeant blocker. We feel the evidence is not sufficient to ascribe the state-dependency to conformational changes in the pore glutamate. Indeed, cysteine accessibility studies for CNGA1 channels have reported that there is no state-dependent change in the rates of covalent modification of a cysteine mutated into this position (E363C; Liu and Siegelbaum 2000). Cysteine substitutions to some residues in the adjacent pore helix do reveal state-dependent changes in rates of covalent modification, suggesting some rotation of this helix during activation (Liu and Siegelbaum 2000; Flynn et al. 2001) and this conformational change could potentially alter the access of channel blockers to the glutamate residue. An alternative possibility for the state dependence of block is that ion permeation (in the open state) inhibits the interactions between positively charged blockers and the negative glutamates. The possibility that the effects of the E342Q mutation are due to nonspecific changes in the pore structure seems unlikely given that the mutation of this residue to alanine does not markedly alter the accessibility of cysteine mutated P-loop residues to modification by Cd^{2+} (Roncaglia and Becchetti 2001). Regardless of the precise mechanism, the closed state dependency for intracellular block suggests the intracellular mouth of the channel pore is wide enough to allow access of large organic cations to the pore and that the putative extracellular vestibule glutamate can interact with nonpermeant intracellular blockers in this closed state.

Acknowledgements We thank Anne Cunningham for the CNGA2 cDNA, originally donated by R. Reed (see "Materials and methods"). The grant support of the Australian Research Council and the NHMRC of Australia is much appreciated.

References

Becchetti A, Gamel K, Torre V (1999) Cyclic nucleotide-gated channels. Pore topology studied through the accessibility of reporter cysteines. J Gen Physiol 114:377–392

Becchetti A, Roncaglia P (2000) Cyclic nucleotide-gated channels: intracellular and extracellular accessibility to Cd^{2+} of substituted cysteine residues within the *P*-loop. Pflügers Arch 440:556–565

Bönigk W, Bradley J, Müller F, Sesti F, Boekhoff I, Ronnett GV, Kaupp UB, Frings S (1999) The native rat olfactory cyclic nucleotide-gated channel is composed of three distinct subunits. J Neurosci 13:5332–5347

Brown L, Haley TL, West KA, Crabb JW (1999) Pseudechetoxin: a peptide blocker of cyclic nucleotide-gated ion channels. Proc Natl Acad Sci USA 96:754–759

Bucossi G, Eismann E, Sesti F, Nizzari M, Seri M, Kaupp UB, Torre V (1996) Time-dependent current decline in cyclic GMP-gated bovine channels caused by point mutations in the pore region expressed in Xenopus oocytes. J Physiol 493:409–418

Castle NA, Haylett DG, Morgan JM, Jenkinson DH (1993) Dequalinium: a potent inhibitor of apamin-sensitive K^+ channels in hepatocytes and of nicotinic responses in skeletal muscle. Eur J Pharmacol 236:201–207

Chen C, Okayama H (1987) High efficiency expression of mammalian cells by plasmid DNA. Mol Cell Biol 7:2745–2751

Corey DP, Stevens CF (1983) Science and technology of patch-recording electrodes. In: Sakmann B, Neher E (eds) Single-channel recording. Plenum Press, New York

Doyle DA, Morais Cabral J, Pfuetzner RA, Kuo A, Gulbis JM, Cohen SL, Chait BT, MacKinnon R (1998) The structure of the potassium channel: molecular basis of K^+ conduction and selectivity. Science 280:69–77

Dunn PM, Benton DC, Campos Rosa J, Ganellin CR, Jenkinson DH (1996) Discrimination between subtypes of apamin-sensitive Ca^{2+} -activated K^+ channels by gallamine and a novel bis-quaternary quinolinium cyclophane, UCL 1530. Br J Pharmacol 117:35–42

Eismann E, Muller F, Heinemann SH, Kaupp UB (1994) A single negative charge within the pore region of a cGMP-gated channel controls rectification, Ca^{2+} blockage, and ionic selectivity. Proc Natl Acad Sci USA 91:1109–1113

Flynn GE, Johnson JP, Zagotta WN (2001) Cyclic nucleotide-gated channels: shedding light on the opening of a channel pore. Nat Rev Neurosci 2(9):643–651

Fodor AA, Gordon SE, Zagotta WN (1997a) Mechanisms of tetracaine block of cyclic nucleotide-gated channels. J Gen Physiol 109:3–14

Fodor AA, Black KD, Zagotta WN (1997b) Tetracaine reports a conformational change in the pore of cyclic nucleotide-gated channels. J Gen Physiol 110(5):591–600

Frings S, Seifert R, Godde M, Kaupp UB (1995) Profoundly different calcium permeation and blockage determine specific function of distinct cyclic nucleotide-gated channels. Neuron 15:169–179

Gavazzo P, Picco C, Eismann E, Kaupp UB, Menini A (2000) A point mutation in the pore region alters gating Ca^{2+} blockage and permeation of olfactory cyclic nucleotide-gated channels. J Gen Physiol 116:311–325

Ghatapande AS, Uma R, Karpen JW (2003) A multiply charged tetracaine derivative blocks cyclic nucleotide-gated channels at subnanomolar concentrations. Biochem 42:265–270

Gordon SE, Zagotta WN (1995) Localization of regions affecting an allosteric transition in cyclic nucleotide-activated channels. Neuron 14:857–864

Gorman CM, Gies DR, McRay G (1990) Transient production of proteins using an adenovirus transformed cell line. DNA Protein Eng Tech 2:3–10

Guo D, Lu Z (2000) Mechanism of cGMP-gated channel block by intracellular polyamines. J Gen Physiol 115:783–797

Hamill OP, Marty A, Neher E, Sakmann B, Sigworth FJ (1981) Improved patch-clamp techniques for high-resolution current recording from cells and cell-free membrane patches. Pflügers Arch 391:85–100

Heginbotham L, Abramson T, MacKinnon R (1992) A functional connection between the pores of distantly related ion channels as revealed by mutant K^+ channels. Science (Washington, DC) 258:1152–1155

Jan LY, Jan YN (1990) A superfamily of ion channels. Nature (Lond) 345(6277):672

Kaupp UB, Niidome T, Tanabe T, Terada S, Bőnigk W, Stuhmer W, Cook NJ, Kangawa K, Matsuo H, Hirose T (1989) Primary structure and functional expression from complementary DNA of the rod photoreceptor cyclic GMP-gated channel. Nature (Lond) 342:762–766

Lancet D (1986) Vertebrate olfactory reception. Annu Rev Neurosci 9:329–355

Liu J, Siegelbaum SA, (2000) Change of pore helix conformational state during opening of cyclic nucleotide-gated channels. Neuron 28:899–909

Lowe G, Gold GH (1993) Nonlinear amplification by calcium-dependent chloride channels in olfactory receptor cells. Nature 366:283–285

Lynch JW (1999) Rectification of the olfactory cyclic nucleotide-gated channel by intracellular polyamines. J Membr Biol 170:213–227

Nevin ST, Haddrill JL, Lynch JW (2000) A pore-lining glutamic acid in the rat olfactory cyclic nucleotide-gated channel controls external spermine block. Neurosci Lett 296(2–3):163–167

Park CS, MacKinnon R (1995) Divalent cation selectivity in a cyclic nucleotide-gated channel. Biochemistry 34:13328–13333

Roncaglia P, Becchetti A (2001) Cyclic-nucleotide-gated channels: pore topology in desensitizing E19A mutants. Pflügers Arch—Eur J Physiol 441:772–780

Root MJ, MacKinnon R (1993) Identification of an external divalent cation-binding site in the pore of a cGMP-activated channel. Neuron 11:459–466

Root MJ, MacKinnon R (1994) Two identical noninteracting sites in an ion channel revealed by proton transfer. Science (Washington, DC) 265:1852–1856

Rosenbaum T, Islas LD, Carlson AE, Gordon SE (2003) Dequalinium: a novel, high-affinity blocker of CNGA1 channels. J Gen Physiol 121(1):37–47

Rosenbaum T, Gordon-Shaag AG, Islas LD, Cooper J, Munari M, Gordon, SE (2004) State-dependent block of CNG channels by dequalinium. J Gen Physiol 123:295–304

Rotenberg SA, Sun XG (1998) Photoinduced inactivation of protein kinase C by dequalinium identifies the RACK-1-binding domain as a recognition site. J Biol Chem 273(4): 2390–2395

Strobaek D, Jorgensen TD, Christophersen P, Ahring PK, Olesen SP (2000) Pharmacological characterization of small-conductance Ca^{2+}-activated K^+ channels stably expressed in HEK293 cells. Br J Pharmacol 129:991–999

Zufall F, Firestein S, Shepherd GM (1994) Cyclic nucleotide-gated ion channels and sensory transduction in olfactory receptor neurons. Annu Rev Biophys Biomol Struct 23:577–607